



CHALMERS
UNIVERSITY OF TECHNOLOGY

Dual Role of Boronic Acid Modification in Enhancing Rheological and Photophysical Properties of Supramolecular Gels

Downloaded from: <https://research.chalmers.se>, 2025-04-27 07:17 UTC

Citation for the original published paper (version of record):

Saha, E., Ruiu, A., Zacharias, S. et al (2024). Dual Role of Boronic Acid Modification in Enhancing Rheological and Photophysical Properties of Supramolecular Gels. *Macromolecules*, 57(7): 3183-3189.
<http://dx.doi.org/10.1021/acs.macromol.3c02091>

N.B. When citing this work, cite the original published paper.

Dual Role of Boronic Acid Modification in Enhancing Rheological and Photophysical Properties of Supramolecular Gels

Ekata Saha, Andrea Ruiu, Savannah C. Zacharias, Anna Ström, and Henrik Sundén*



Cite This: <https://doi.org/10.1021/acs.macromol.3c02091>



Read Online

ACCESS |



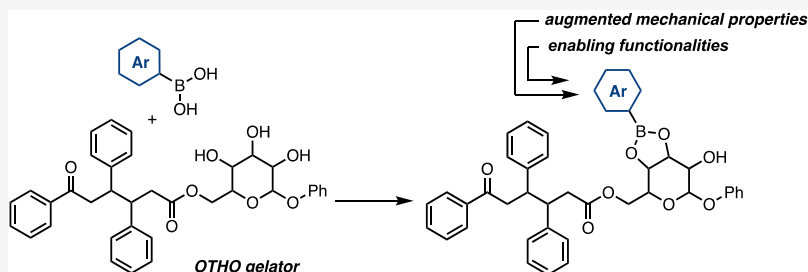
Metrics & More



Article Recommendations



Supporting Information



ABSTRACT: Supramolecular gels derived from functionalized gelators offer diverse applications, and modifying the properties of existing organogels using guest molecules presents an attractive approach for designing functional gel materials with targeted properties. In this study, we investigated a method to enhance the mechanical and photophysical properties of readily prepared low molecular weight gels (LMWGs) through the incorporation of boronic acid derivatives. The leveraging of dynamic covalent bonding interactions between the hydroxyl groups of oxotriphenylhexanoates (OTHO) gelator and the boronic acid derivatives gave rise to a boronate adduct along with enhanced intermolecular aromatic stacking interactions between gelators and thereby reinforced the rheological and thermal stability of the doped OTHO gels. In an effort to probe the aforementioned aromatic interactions, we used a pyrene boronic acid dopant, which revealed that the spatial proximity between the aromatic groups of the boronic acid was close enough to display excimer formation. Our findings provide valuable insights into the regulation of mechanical strength, self-healing ability, and photophysical properties of supramolecular gels. Furthermore, this approach holds promise for broad applications in hydroxyl-containing LMWGs, enabling the development of functional gel materials with enhanced properties.

INTRODUCTION

Supramolecular gels based on low molecular weight gelators (LMWGs) have received widespread attention owing to the easy tunability of their structure and numerous prospective applications in multidisciplinary fields¹ including, self-healing materials,² rewritable materials,³ wound healing,⁴ drug delivery,⁵ optoelectronics,⁶ sensing,⁷ imaging,^{8,9} environmental remediation,¹⁰ catalysis,¹¹ and renewable energy applications.¹² The high structural tunability arises from the simple fact that a gelator based on a small molecule is easier to modify (to decorate with the desired functionality) than the polymer counterpart. Polymers are constructed through covalent bonds among the network components, whereas supramolecular gels are formed through noncovalent interactions, including hydrogen bonding, π - π stacking, van der Waals forces, electrostatic interactions, and aromatic interactions.¹³ However, the absence of covalent bonds between the network components typically results in the inherent mechanical fragility of supramolecular gels, causing them to break at low strain levels. This limitation restricts their use in various applications. Significant efforts comprising different chemical,¹⁴ physical¹⁵ and enzymatic¹⁶ cross-linking approaches have been devoted to tuning the mechanical properties of supramolecular

gels. The most common methods are the addition of metal ions,¹⁷ photoinduced cross-linking,¹⁸ incorporation of charge transfer interactions,¹⁹ inorganic composites,²⁰ and biomacromolecules²¹ to strengthen the gels. These methods permit an improvement of the mechanical stability of the gel; nevertheless, remarkable structural alteration of the network component is involved. An alternative method is to install reactive functional groups on the gelator,²² allowing an intermolecular covalent cross-linking of the gel fibers. For example, condensation between hydrazide and amino groups with aldehyde cross-linkers has been investigated.^{23,24} All of the aforementioned methods require either challenging LMWG design and/or lead to supramolecular structural modification.

In recent decades, sugar-based organogelators have been heavily explored for advanced applications.^{25–30} Sugars are

Received: October 16, 2023

Revised: March 9, 2024

Accepted: March 12, 2024

well-known to quickly react with boron-based acids through hydroxylic groups to form boronic esters (boronates). The reactivity of boronic esters is commonly used in organic synthesis but has also been used in biological science.^{31–36} Furthermore, the reactivity between hydroxyls and boronic acids has been investigated in macromolecular chemistry, allowing the functionalization of polymers, their cross-linking, and thereby the tuning of the rheological properties.³⁷ Moreover, boronic acid-based small molecules have also been investigated as gelators.^{38–43} For example (arylboronate alkylglucoside)-based organogels derived from alkylglucosides with aryl boronic acids were reported recently, but the study was focused on the sensitivity of the boronate function toward hydrolysis.^{44,45} However, to the best of our knowledge, the bifunctional role of boron derivatives in improving mechanical properties and modulating the photophysical properties has not been tested or evaluated for supramolecular gels based on LMWGs to date.

Recently, we reported on the synthesis and gel properties of oxotriphenylhexanoates (OTHOs).⁴⁶ The OTHO gelator is a versatile gelator that is capable of gelation in a number of solvents including water.^{47,48} Moreover, the OTHO can be functionalized and used in photonic applications⁴⁹ and catalysis.¹¹ Furthermore, the OTHO can be easily combined with a sugar-based glycopyranoside substituent to form a transparent organogel (OTHO1) at a low concentration (<2 wt %) (Figure 1a). The primary objective of this study is to

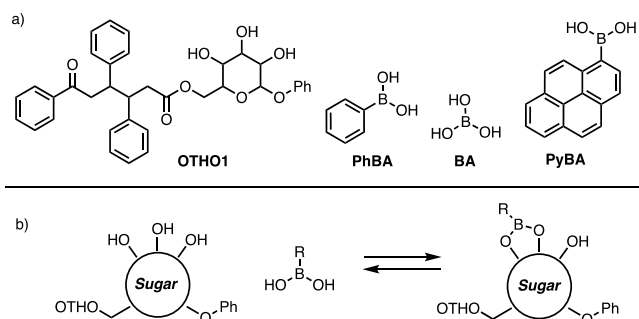


Figure 1. (a) Molecular structure of the OTHO1 gelator, PhBA, BA, and PyBA. (b) General model for the dynamic covalent bonding interactions proposed for OTHO1 in the presence of boron acid species.^{50,51}

develop a facile method for achieving dynamic cross-linking of supramolecular structures (Figure 1b) by means of a simple modulation process involving different components capable of interacting with one another, thereby forming a bicomponent supramolecular network. This approach eliminates the need for complex molecular design, lengthy synthetic procedures, and laborious purification steps. Instead, it entails the straightforward addition of commercially available boron-based acids, such as boric acid (BA), phenylboronic acid (PhBA), and pyrene-1-boronic acid (PyBA) to the sugar-based OTHO1 gelator (or other hydroxyl-containing gelators) leading to the formation of readily prepared doped gels. Building upon this concept, we have systematically investigated the effects of varying molar ratios of BA, PhBA, and PyBA on the morphological, thermal, and rheological properties of OTHO1 gels (Figure 1).

RESULTS AND DISCUSSION

The organogels were prepared by mixing a 15 mg/mL solution of OTHO1 gelator with varying amounts of boron-based acid species in toluene. The mixture was heated until complete solubilization of the components was achieved, followed by sonication to induce gel formation. It should be noted that a higher loading of PhBA leads to the formation of a thick precipitate in toluene, thereby diminishing the capacity to interact with the OTHO1 gelator. However, up to 8 equiv of the boronic acids can be employed to achieve reproducible gelation for our systems.

We have recorded the SEM images of the corresponding gel-derived xerogels obtained from the OTHO1 gel as well as the modified OTHO1 gels with PhBA (OTHO1-PhBA), BA (OTHO1-BA), and PyBA (OTHO1-PyBA) in order to gain an insight into the microstructure of the gels (Figures 2 and S1–S4). All four gels afforded entangled fibrous structure on the micrometer scale (with no visual phase separation).

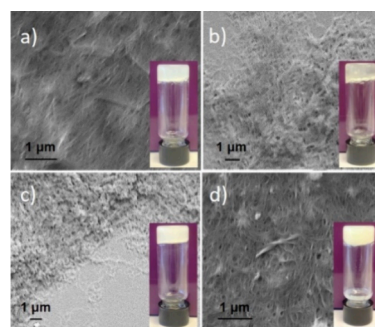


Figure 2. SEM images of (a) OTHO1, (b) OTHO1-PhBA, (c) OTHO1-BA, and (d) OTHO1-PyBA xerogels. Photographs of the organogels OTHO1, OTHO1-PhBA and OTHO1-BA and OTHO1-PyBA are provided as the corresponding inset images.

Thermal studies, TGA (Figures S5 and S6, Table S1) and DSC (Figures S7 and S8), show the modification of the thermal properties of the xerogels after doping. TGA profiles showed us the temperature-induced degradation pathways and how the structural variation of boronic acids affects the unique thermal stability trends of our gel systems. OTHO1-xerogel has an onset degradation temperature of ~ 224 °C. In comparison, xerogels of OTHO1-BA, OTHO1-PhBA, and OTHO1-PyBA have onset degradation temperatures at ~ 116 , 239, and 237 °C respectively. For OTHO1-PhBA and OTHO1-PyBA xerogels, this elevated onset degradation temperature is attributed to the increased thermal stability due to the formation of the corresponding boronic esters. For the OTHO1-BA xerogel, we did not observe any significant changes in the onset degradation temperature compared to BA indicating that the hybrid system is not contributing to the thermal stability. In the DSC data, we observed a clear thermal event for the PhBA at ~ 80 °C attributing to a dehydration event.^{52,53} In the case of the OTHO1-PhBA xerogel, we observed a similar thermal event at a much higher temperature indicating that the boronic ester formed during gel formation is more thermally stable than the parent boronic acid.

The modification in thermal stability is attributed to the involvement of two of the hydroxyls of the OTHO1 in the dynamic covalent formation of a boronic ester (Figure 1b) which can be seen as the general decrease of the intensity of the OH band in OTHO1-dopant xerogel, in the region

between 3500 and 3000 cm^{-1} when comparing the FT-IR spectra (Figures 3 and S9–S11).⁵⁴ For example, PhBA shows a

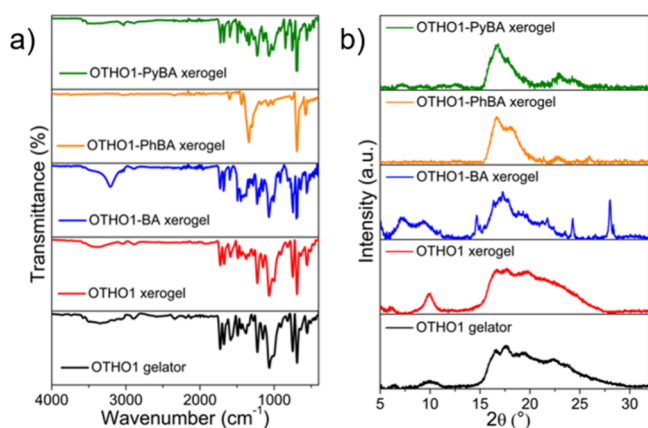


Figure 3. FT-IR spectra (a) and PXRD patterns (b) of the OTHO1 gelator and xerogels.

similar stretching band at 3300 cm^{-1} , due to the hydroxyl of the boronic acid (Figures 3 and S9). A weak band at 3300 cm^{-1} in the OTHO1-PhBA solid mixture indicates a starting interaction between the PhBA and the sugar hydroxyl of the OTHO1 gelator. Finally, the spectrum of the OTHO1-PhBA xerogel shows a complete disappearance of the OH signal owing to the formation of a boronic ester bond via the dynamic covalent cross-linking interactions between OTHO1 and the PhBA moiety. Similar phenomena were observed for the OTHO1-BA and OTHO1-PyBA gels (Figures S10 and S11). The experimental PXRD pattern of the OTHO1-dopant xerogel is not a sum of the patterns of the starting materials, indicating a new phase has been formed (Figures 3 and S12–S14). The differences confirm the interactions between the OTHO1 and the dopants.

To verify the formation of the OTHO1-boronic ester adduct, we subjected our OTHO1-PhBA xerogel to high-resolution mass analysis (Figure S15) and could identify the formed ester species. After the interactions between the gelator and the dopants were confirmed, rheological studies (Figures 4

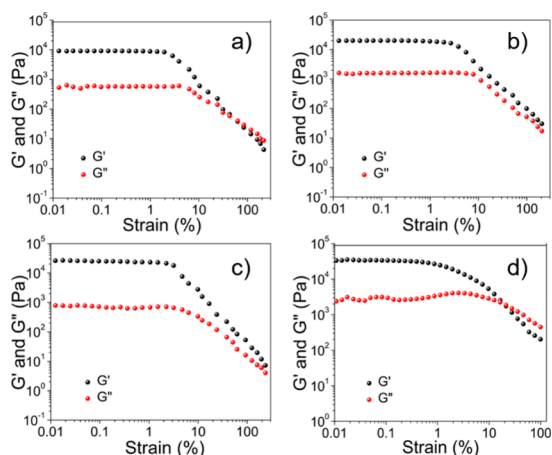


Figure 4. Oscillatory rheological measurements of the gels. Strain sweep experiments for (a) OTHO1, (b) OTHO1-BA (BA: 8 equiv), (c) OTHO1-PhBA (PhBA: 8 equiv) and (d) OTHO1-PyBA (PyBA: 4 equiv) gels.

and S16–S42) were conducted to examine the impact of the boron additives on the rheological properties of the materials. The doped gels (with 1, 4, and 8 equiv of boron-based acids) and undoped gels were analyzed to investigate the alterations in the rheological properties resulting from the presence or absence of the boron additives. Dynamic rheological experiments on the gels confirmed their viscoelastic gel nature. At low strain, the storage modulus (G' , the elastic contribution) was significantly higher than the loss modulus (G'' , the viscous contribution). OTHO1 gels doped with different equivalents (1, 4, and 8) of boron species were tested during the rheological measurements (Table 1). Strain sweep illustrated a

Table 1. Data Related to the Strain Sweep Measurements of the Organogels As Determined at a Frequency of 6.28 rad/s and $T = 20\text{ }^\circ\text{C}$

gel	equiv of boron species added	G' (kPa)	G'' (kPa)	$\tan \delta$ (G''/G')	yield point (strain%)
OTHO1		9	1.5	0.17	1.06
OTHO1-BA	1	8.6	0.9	0.1	0.41
	4	11.7	1.1	0.09	0.59
	8	20.3	1.3	0.06	0.64
OTHO1-PhBA	1	16.9	0.7	0.04	0.57
	4	20.5	0.6	0.03	0.71
	8	26.0	0.8	0.03	1.81
OTHO1-PyBA	1	14.7	1.8	0.12	0.70
	4	39.2	2.1	0.05	1.13

linear viscoelastic (LVE) region at low deformation of both doped and undoped gels. The increasing amount of boron additive, for both OTHO1-BA and OTHO1-PhBA gels, leads to the rise of G' (Figures S16–S24). The OTHO1 gel has a G' equal to 9 kPa, which can be improved to 11.7 and 20.3 kPa by the addition of BA, for the 4 and 8 equiv boron species-based systems, respectively. A similar trend is observed for the increasing amount of PhBA. In this case, upon the addition of 1 equiv of PhBA the G' rises to 16.9 kPa, which is almost twice the strength of the OTHO1 gel. The G' value was further improved by the addition of 4 and 8 equiv of PhBA, resulting in a G' of 20.5 and 26 kPa, respectively. In the case of OTHO1-PyBA gel, the G' values were observed to be 14.7 and 39.2 kPa for 1 and 4 equiv of PyBA, respectively. Since the G'' remains almost constant for the hybrid and pure systems (Figure 4), showing a substantial increase in elastic component contribution to the network through the addition of the dopant. The $\tan \delta$ ($\tan \delta = G''/G'$) values were observed below 1 indicating the solid-like nature of the gels. On the other hand, decreasing $\tan \delta$ with an increase in boron dopants indicates that the doped gels act more elastic in nature. Furthermore, the OTHO1 gel has a yield point of 1.06%, indicating a certain resistance to the strain stress before the supramolecular systems start to suffer structural modification (Figure S25). This value is observed in the range of 0.41–1.81% for the hybrid systems (Figures S26–S33). Frequency sweep measurements (Figures S34–S42) displayed minimum dependence of G' on frequency over the experimental region. G' exceeded G'' by an order of magnitude corroborates the viscoelastic gel-like behavior. The overall pattern of the G' and G'' were similar for the original and hybrid OTHO1 gels; however, the G' of the OTHO1-PhBA gel was larger compared to the OTHO1 gel. This confirms the more elastic nature of the OTHO1-PhBA gel than the OTHO1 gel. The OTHO1-

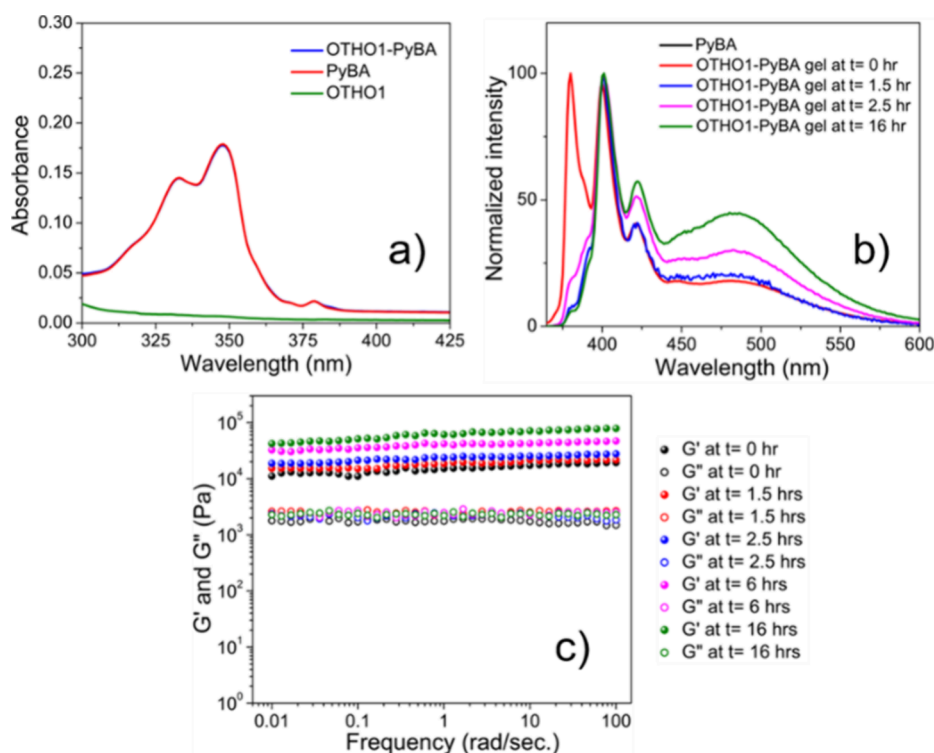


Figure 5. (a) UV-vis absorption spectra of OTHO1, PyBA, and OTHO1-PyBA gel with 1 equiv PyBA; (b) fluorescence emission spectra of OTHO1-PyBA gel throughout the gelation process (with respect to time) ($\lambda_{\text{ex}} = 348 \text{ nm}$). 2 mg of the gel was thoroughly dispersed in 2 mL of toluene for all spectroscopic measurements. (c) Frequency sweep experiments conducted at different time intervals after gelation for the OTHO1-PyBA gel (with 1 equiv of PyBA) to shed light on the influence of gel aging up on the typical trend of G' and G'' values.

PyBA gel corresponds to similarly high G' values like the OTHO1-PhBA gel; however, the former one shows higher $\tan \delta$ values. This observation can be attributed to a higher elastic component but a more fluid-like behavior of OTHO1-PyBA gel at high-strain amplitudes ($G'' > G'$) unlike the other three gels. These results indicate that the hybrid organogels are characterized by a larger amount of network formation, suggesting a higher cross-linking due to the presence of the boron species.

For practical applications of supramolecular gels, the self-healing ability of the material represents a key factor, worthy of investigation due to their ability to repair their structure and properties in response to damage. Time-dependent hysteresis loop tests (dynamic step-strain measurements) were performed (Figures S43–S46) to monitor the thixotropic behavior of both the pristine and doped gels by alternating low and high strain at certain time intervals at a constant oscillation frequency of 6.28 rad/s for realizing the gel-to-sol ($G'' > G'$) and sol-to-gel ($G' > G''$) conversions. Interestingly, the original strengths of the gels were recovered almost instantaneously when the breaking strain was removed. At first, the gels were subjected to a constant strain of 0.01% and then the strain was increased to 250% (100% for OTHO1-PyBA gel) and then again decreased to 0.01%, and the entire step was repeated for 3 cycles for OTHO1 gel and 5 cycles for doped OTHO1 gels. The OTHO1 organogel showed a relatively good self-healing ability, resulting in a gel able to recover most of the storage modulus (62% of its original strength) at the end of the three consecutive step-strain cycles. The OTHO1-BA gel recovered 39 and 27% of its original strength immediately after the first cycle and after five consecutive cycles, respectively. Surprisingly, the OTHO1-PhBA and OTHO1-

PyBA gels recovered 92 and 83% of their initial strength, respectively, even after five successive step-strain cycles, indicating a rapid, repeatable, and autonomous self-healing behavior of the gels. The lower self-healing ability of OTHO1-BA gel can be attributed to partial unreacted BA present in the supramolecular gel pockets as evidenced from the PXRD pattern (Figure S13).

The different results obtained from the OTHO1-BA and OTHO1-PhBA gels indicated different strengthening processes for these additives. Starting from the BA system, its solubilization in toluene is not favorable so higher temperatures are necessary ($\sim 100 \text{ }^\circ\text{C}$). Nevertheless, these can lead to a rearrangement of the boron compound, going from the crystalline structure of BA to the amorphous B_2O_3 polymeric system, with lower availability of the key hydroxyl group.⁵⁵ This system would still be able to be integrated into the supramolecular assembly and reinforce the OTHO1 gel system. However, these interactions are weak. The consecutive steps performed in step-strain measurements lead to a gradual reduction of self-healing properties and reaching a behavior like the unreinforced OTHO1 gel. Considering these results, it is possible to affirm that a low compatible compound in an organic solvent like the BA leads to a low interaction process. These can be then overcome and lead to a boron system reorganization and segregation on a molecular scale. The final segregated boron species cannot then keep reinforcing the OTHO1 supramolecular assembly. On the other hand, the PhBA is highly soluble in toluene (also characterized by higher thermal stability) and can easily undergo dynamic covalent bonding interactions in the supramolecular system by means of esterification with the OTHO1 hydroxyl. This dynamism allows an increase of strength and thixotropic ability of

OTHO1-PhBA gel, as an uninterrupted (continuous) and escalated aromatic interaction is possible. This behavior will contribute to keeping the reinforcer role along with exhibiting self-restoring properties of the gel even after the successive steps of loading and unloading external stress as observed in the step-strain experiment.

In general, characterizing aggregation in a multicomponent gel is usually challenging since self-assembled gelation is a complex process involving several noncovalent interactions. The UV–vis absorption spectrum (Figures S4a and S47) of the OTHO1 gel with PyBA is identical to that of the guest molecule, having intense bands in the UV region (two shoulder peaks at ~ 332 and 347 nm) corresponding to the π – π^* transition. The fluorescence emission spectrum of PyBA in a dilute toluene solution is characterized by vibronic bands at ~ 379 , 388 , 399 , and 420 nm, respectively, which are attributed to the π – π^* transitions and entitled as monomeric emission (Figures S4b and S47). In monitoring the fluorescence of OTHO1-PyBA gel, the gel exhibited a similar emission pattern to its doped guest compound. In addition to the monomeric family of bands, a significant broad band appeared at ~ 482 nm due to excited state dimer or excimer emission. The extent of pyrene excimer fluorescence emission is a reflector of distance and flexibility effectuating a favorable interaction between the ground state and excited state pyrene rings. These interactions between the aromatic moieties help in reinforcing the gel (corroborated by rheological analysis). Excimer emission generally arises in a dose-dependent (high concentration) manner;⁵⁶ however, the OTHO1-PyBA gel showed an increase in excimer emission intensity upon aging at room temperature from 0 to 16 h (Figure S48). From the observation of fluorescence intensity over time, we can infer that the interactions or binding of PyBA with the OTHO1 gelator increases with time and the overall emission intensity increases upon achieving a more favorable orientation between the stacked self-assembled motifs. This monotonic increase in the emission intensity can also be attributed to the progressive rigidification (or restriction of movement) of the neighboring environment in the gel network with time. The gel network becomes stronger (higher elastic component contribution), more ordered, and more cross-linked upon aging (Figure S4c) and experiences steric hindrance and thus induces an increased fluorescence emission. This environment-sensitive fluorescence pattern indicates a time-dependent stiffening process of the PyBA-doped gel. The augmentation in gel rigidity was established from the strain and frequency sweeps at different time intervals after gelation for the OTHO1-PyBA gel to shed light on the influence of gel aging upon the typical trend of G' and G'' values (Figures S49–S53, Table S2). Hence, the photophysical response of OTHO1-PyBA gel delineates that the PyBA units are favorably aligning with time and these aromatic interactions thereby reinforce the self-spanning gel network.

CONCLUSIONS

In summary, a series of boron-based acid-doped OTHO1 gels were readily prepared in one step from oxotriphenylhexanoates and boronic acids or boric acid. The rheological and morphological properties of the organogels were determined for each gel. The organogelators self-assembled within the solvent to afford an intertwined fiber-like appearance (observed by SEM). In addition to the preparation and characterization of these organogels, we have demonstrated

that it is possible to utilize a single organogelator to ameliorate the rheological and photophysical properties of the OTHO1 gel depending on the nature of guest boron species (dopants). The approach of mixing boron-based acids with LMWGs containing a hydroxyl group represents a straightforward method to improve the rheological properties of the gels. For example, the addition of PhBA permits a 3 and 4-fold increment of the organogel strength, respectively, together with improved self-healing performance, compared with those measured for the OTHO1 gel without reinforcement. The present study suggests that the improved rheological and thermal stability of the doped OTHO1 gels is the result of covalent bonding interactions between OTHO1 and the boronic acid derivatives, leading to a boronate adduct along with enhanced intermolecular aromatic stacking interactions between gelators. In an attempt to probe the aforesaid aromatic interactions, we used a pyrene boronic acid dopant which was able to indicate that the aromatic groups of the boronic acid are spatially close enough to display excimer formation. The tuning of OTHO1 gel properties by varying the guest molecules manifests the importance of unique structural relationships and nonbonding interactions in designing LMWGs, which commits to the ongoing efforts to determine the structural features of a gelator responsible for gelation. The study of different boron unit-incorporated sugar gelators with advantageous refinement properties can lead to novel supramolecular gels with desirable rheological and photophysical properties for real-life applications.

ASSOCIATED CONTENT

Supporting Information

The Supporting Information is available free of charge at <https://pubs.acs.org/doi/10.1021/acs.macromol.3c02091>.

Materials and methods, detailed synthesis, gelation procedure, and material characterizations and results (PDF)

AUTHOR INFORMATION

Corresponding Author

Henrik Sundén – Department of Chemistry and Molecular Biology, University of Gothenburg, 405 30 Gothenburg, Sweden; orcid.org/0000-0001-6202-7557; Email: henrik.sunden@chem.gu.se

Authors

Ekata Saha – Department of Chemistry and Molecular Biology, University of Gothenburg, 405 30 Gothenburg, Sweden

Andrea Ruiu – Department of Chemistry and Molecular Biology, University of Gothenburg, 405 30 Gothenburg, Sweden

Savannah C. Zacharias – Department of Chemistry and Molecular Biology, University of Gothenburg, 405 30 Gothenburg, Sweden

Anna Ström – Department of Chemistry and Chemical Engineering, Chalmers University of Technology, 412 96 Gothenburg, Sweden; orcid.org/0000-0002-9743-1514

Complete contact information is available at: <https://pubs.acs.org/doi/10.1021/acs.macromol.3c02091>

Author Contributions

E.S.: Methodology, formal analysis, data curation (characterization), validation, writing original draft, review, and editing. A.R.: methodology, data curation (synthesis and characterization), writing. S.C.Z.: analysis, methodology, data curation (PXRD, FT-IR), and review. A.S.: data validation (rheology), review and editing. HS: Formulation of research question, fund acquisition, supervision, review, and editing. The manuscript was written through contributions of all authors. All authors have given approval to the final version of the manuscript. E.S. and A.R. authors contributed equally.

Funding

The authors are grateful for financial support of this work by the Wenner-Gren Foundation Grant (#UP2020-0208) and Olle Engkvists stiftelse (#217-0037).

Notes

The authors declare no competing financial interest.

REFERENCES

- (1) Adams, D. J. Personal Perspective on Understanding Low Molecular Weight Gels. *J. Am. Chem. Soc.* **2022**, *144*, 11047–11053.
- (2) Strandman, S.; Zhu, X. X. Self-Healing Supramolecular Hydrogels Based on Reversible Physical Interactions. *Gels* **2016**, *2*, 16.
- (3) Lin, Q.; Zheng, F.; Lu, T. T.; Liu, J.; Li, H.; Wei, T. B.; Yao, H.; Zhang, Y. M. A novel imidazophenazine-based metallogel act as reversible H_2PO_4^- sensor and rewritable fluorescent display material. *Sens. Actuators B Chem.* **2017**, *251*, 250–255.
- (4) Chen, C.; Yang, X.; Li, S. J.; Zhang, C.; Ma, Y. N.; Ma, Y. X.; Gao, P.; Gao, S. Z.; Huang, X. J. Tannic acid–thioctic acid hydrogel: a novel injectable supramolecular adhesive gel for wound healing. *Green Chem.* **2021**, *23*, 1794–1804.
- (5) Raymond, D. M.; Abraham, B. L.; Fujita, T.; Watrous, M. J.; Toriki, E. S.; Takano, T.; Nilsson, B. L. Low-Molecular-Weight Supramolecular Hydrogels for Sustained and Localized in Vivo Drug Delivery. *ACS Appl. Bio Mater.* **2019**, *2*, 2116–2124.
- (6) Cross, E. R.; Sproules, S.; Schweins, R.; Draper, E. R.; Adams, D. J. Controlled Tuning of the Properties in Optoelectronic Self-Sorted Gels. *J. Am. Chem. Soc.* **2018**, *140*, 8667–8670.
- (7) Gao, A.; Han, Q.; Wang, Q.; Wan, R.; Wu, H.; Cao, X. Bis-Pyridine-Based Organogel with AIE Effect and Sensing Performance towards Hg^{2+} . *Gels* **2022**, *8*, 464.
- (8) Roy, R.; Dastidar, P. Multidrug-Containing, Salt-Based, Injectable Supramolecular Gels for Self-Delivery, Cell Imaging and Other Materials Applications. *Eur. J. Chem.* **2016**, *22*, 14929–14939.
- (9) Majumder, L.; Chatterjee, M.; Bera, K.; Maiti, N. C.; Banerji, B. Solvent-Assisted Tyrosine-Based Dipeptide Forms Low-Molecular Weight Gel: Preparation and Its Potential Use in Dye Removal and Oil Spillage Separation from Water. *ACS Omega* **2019**, *4*, 14411–14419.
- (10) Okesola, B. O.; Smith, D. K. Applying low-molecular weight supramolecular gelators in an environmental setting – self-assembled gels as smart materials for pollutant removal. *Chem. Soc. Rev.* **2016**, *45*, 4226–4251.
- (11) Zacharias, S. C.; Kamlar, M.; Sundén, H. Exploring Supramolecular Gels in Flow-Type Chemistry—Design and Preparation of Stationary Phases. *Ind. Eng. Chem. Res.* **2021**, *60*, 10056–10063.
- (12) Saha, E.; Karthick, K.; Kundu, S.; Mitra, J. Electrocatalytic Oxygen Evolution in Acidic and Alkaline Media by a Multistimuli-Responsive Cobalt(II) Organogel. *ACS Sustain. Chem. Eng.* **2019**, *7*, 16094–16102.
- (13) Weiss, R. G. The past, present, and future of molecular gels. What is the status of the field, and where is it going? *J. Am. Chem. Soc.* **2014**, *136*, 7519–7530.
- (14) Marshall, L. J.; Matsarskaia, O.; Schweins, R.; Adams, D. J. Enhancement of the mechanical properties of lysine-containing peptide-based supramolecular hydrogels by chemical cross-linking. *Soft Matter* **2021**, *17*, 8459–8464.
- (15) Zhang, X.; Chu, X.; Wang, L.; Wang, H.; Liang, G.; Zhang, J.; Long, J.; Yang, Z. Rational Design of a Tetrameric Protein to Enhance Interactions between Self-Assembled Fibers Gives Molecular Hydrogels. *Angew. Chem., Int. Ed.* **2012**, *51*, 4388–4392.
- (16) Li, Y.; Ding, Y.; Qin, M.; Cao, Y.; Wang, W. An enzyme-assisted nanoparticle crosslinking approach to enhance the mechanical strength of peptide-based supramolecular hydrogels. *ChemComm* **2013**, *49*, 8653–8655.
- (17) Park, J.; Kim, K. Y.; Kim, C.; Lee, J. H.; Kim, J. H.; Lee, S. S.; Choi, Y.; Jung, J. H. A crown-ether-based moldable supramolecular gel with unusual mechanical properties and controllable electrical conductivity prepared by cation-mediated cross-linking. *Polym. Chem.* **2018**, *9*, 3900–3907.
- (18) Yabuuchi, K.; Matsuo, N.; Maeda, H.; Moriyama, M. Photoinduced reinforcement of supramolecular gels based on a coumarin-containing gelator. *Polym. J.* **2018**, *50*, 1093–1097.
- (19) Yang, Z.; Li, Y.; Shen, C.; Chen, Y.; Li, H.; Zhou, A.; Liu, K. Tuning Rheological Behaviors of Supramolecular Aqueous Gels via Charge Transfer Interactions. *Langmuir* **2021**, *37*, 14713–14723.
- (20) Nanda, J.; Biswas, A.; Adhikari, B.; Banerjee, A. A Gel-Based Trihybrid System Containing Nanofibers, Nanosheets, and Nanoparticles: Modulation of the Rheological Property and Catalysis. *Angew. Chem., Int. Ed.* **2013**, *52*, 5041–5045.
- (21) Li, D.; Wang, H.; Kong, D.; Yang, Z. BSA-stabilized molecular hydrogels of a hydrophobic compound. *Nanoscale* **2012**, *4*, 3047–3049.
- (22) Zhang, J.-Y.; Zeng, L.-H.; Feng, J. Dynamic covalent gels assembled from small molecules: from discrete gelators to dynamic covalent polymers. *Chin. Chem. Lett.* **2017**, *28*, 168–183.
- (23) Noteborn, W. E. M.; Zwagerman, D. N. H.; Talens, V. S.; Maity, C.; van der Mee, L.; Poolman, J. M.; Mytnyk, S.; van Esch, J. H.; Kros, A.; Eelkema, R.; Kieleyka, R. E. Crosslinker-Induced Effects on the Gelation Pathway of a Low Molecular Weight Hydrogel. *Adv. Mater.* **2017**, *29*, 1603769.
- (24) Khalily, M. A.; Goktas, M.; Guler, M. O. Tuning viscoelastic properties of supramolecular peptide gels via dynamic covalent crosslinking. *Org. Biomol. Chem.* **2015**, *13*, 1983–1987.
- (25) Morris, J.; Bietsch, J.; Bashaw, K.; Wang, G. Recently Developed Carbohydrate Based Gelators and Their Applications. *Gels* **2021**, *7*, 24.
- (26) Friggeri, A.; Gronwald, O.; Van Bommel, K. J.; Shinkai, S.; Reinhoudt, D. N. Charge-Transfer Phenomena in Novel, Dual-Component. *Sugar-Based Organogels. J. Am. Chem. Soc.* **2002**, *124*, 10754–10758.
- (27) Luboradzki, R.; Gronwald, O.; Ikeda, A.; Shinkai, S. Sugar-Integrated “Supergelators” Which Can Form Organogels with 0.03–0.05% [g mL⁻¹]. *Chem. Lett.* **2000**, *29*, 1148–1149.
- (28) Prathap, A.; Sureshan, K. M. Sugar-Based Organogelators for Various Applications. *Langmuir* **2019**, *35*, 6005–6014.
- (29) Marr, P. C.; McBride, K.; Evans, R. C. Sugar-derived organogels as templates for structured, photoluminescent conjugated polymer-inorganic hybrid materials. *ChemComm* **2013**, *49*, 6155–6157.
- (30) John, G.; Zhu, G.; Li, J.; Dordick, J. S. Enzymatically Derived Sugar-Containing Self-Assembled Organogels with Nanostructured Morphologies. *Angew. Chem.* **2006**, *118*, 4890–4893.
- (31) Sugita, K.; Tsuchido, Y.; Kasahara, C.; Casulli, M. A.; Fujiwara, S.; Hashimoto, T.; Hayashita, T. Selective Sugar Recognition by Anthracene-Type Boronic Acid Fluorophore/Cyclodextrin Supramolecular Complex Under Physiological pH Condition. *Front. Chem.* **2019**, *7*, 806.
- (32) Imperio, D.; Del Grosso, E.; Fallarini, S.; Lombardi, G.; Panza, L. Synthesis of Sugar-Boronic Acid Derivatives: A Class of Potential Agents for Boron Neutron Capture Therapy. *Org. Lett.* **2017**, *19*, 1678–1681.
- (33) Geethanjali, H. S.; Melavanki, R. M.; Nagaraja, D.; Bhavya, P.; Kusanur, R. A. Binding of boronic acids with sugars in aqueous solution at physiological pH - Estimation of association and

- dissociation constants using spectroscopic method. *J. Mol. Liq.* **2017**, *227*, 37–43.
- (34) Melavanki, R.; Kusanur, R.; Sadasivuni, K. K.; Singh, D.; Patil, N. R. Investigation of interaction between boronic acids and sugar: effect of structural change of sugars on binding affinity using steady state and time resolved fluorescence spectroscopy and molecular docking. *Heliyon* **2020**, *6*, No. e05081.
- (35) Cambre, J. N.; Roy, D.; Sumerlin, B. S. Tuning the sugar-response of boronic acid block copolymers. *J. Polym. Sci. Part A. Polym. Chem.* **2012**, *50*, 3373–3382.
- (36) Maroju, P. A.; Ganesan, R.; Ray Dutta, J. Boronic acid chemistry for fluorescence-based quantitative DNA sensing. *ChemComm* **2022**, *58*, 7936–7939.
- (37) Peters, G. M.; Skala, L. P.; Plank, T. N.; Oh, H.; Reddy, G. N. M.; Marsh, A.; Brown, S. P.; Raghavan, S. R.; Davis, J. T. G4-Quartet- M^+ Borate Hydrogels. *J. Am. Chem. Soc.* **2015**, *137*, 5819–5827.
- (38) Kimura, T.; Shinkai, S. Chirality-dependent Gel Formation from Sugars and Boronic-acid-appended Chiral Amphiphiles. *Chem. Lett.* **1998**, *27*, 1035–1036.
- (39) Inoue, K.; Ono, Y.; Kanekiyo, Y.; Ishi-I, T.; Yoshihara, K.; Shinkai, S. Chiroselective re-binding of saccharides to the fibrous aggregates prepared from organic gels of cholesterylphenylboronic acid. *Tetrahedron Lett.* **1998**, *39*, 2981–2984.
- (40) Kubo, Y.; Yoshizumi, W.; Minami, T. Development of Chemical Stimuli-responsive Organogel Using Boronate Ester-substituted Cyclotricatechylene. *Chem. Lett.* **2008**, *37*, 1238–1239.
- (41) Grigoriou, S.; Johnson, E. K.; Chen, L.; Adams, D. J.; James, T. D.; Cameron, P. J. Dipeptide hydrogel formation triggered by boronic acid–sugar recognition. *Soft Matter* **2012**, *8*, 6788–6791.
- (42) Mahendar, C.; Dixit, M. K.; Kumar, Y.; Dubey, M. d-(+)-Glucose-triggered metallogel to metallogel transition. *J. Mater. Chem. C* **2020**, *8*, 11008–11012.
- (43) Daniels, E. L.; Runge, J. R.; Oshinowo, M.; Leese, H. S.; Buchard, A. Cross-Linking of Sugar-Derived Polyethers and Boronic Acids for Renewable, Self-Healing, and Single-Ion Conducting Organogel Polymer Electrolytes. *ACS Appl. Energy Mater.* **2023**, *6*, 2924–2935.
- (44) Ludwig, A. D.; Saint-Jalmes, A.; Mériadec, C.; Artzner, F.; Tasseau, O.; Berrée, F.; Lemiègre, L. Boron Effect on Sugar-Based Organogelators. *Chem.—Eur. J.* **2020**, *26*, 13927–13934.
- (45) Ludwig, A. D.; Ourvois-Maloisel, N.; Saint-Jalmes, A.; Artzner, F.; Guégan, J. P.; Tasseau, O.; Berrée, F.; Lemiègre, L. Adjusting the water-sensitivity of sugar/boronate-based organogels. *Soft Matter* **2022**, *18*, 9026–9036.
- (46) Ta, L.; Axelsson, A.; Bijl, J.; Haukka, M.; Sundén, H. Ionic Liquids as Precatalysts in the Highly Stereoselective Conjugate Addition of α,β -Unsaturated Aldehydes to Chalcones. *Chem. - A Eur. J.* **2014**, *20*, 13889–13893.
- (47) Hsu, C.-W.; Sauvée, C.; Sundén, H.; Andréasson, J. Writing and erasing multicolored information in diarylethene-based supramolecular gels. *Chem. Sci.* **2018**, *9*, 8019–8023.
- (48) Sauvée, C.; Ström, A.; Haukka, M.; Sundén, H. A Multi-Component Reaction towards the Development of Highly Modular Hydrogelators. *Chem. - A Eur. J.* **2018**, *24*, 8071–8075.
- (49) Johnstone, M. D.; Hsu, C. W.; Hochbaum, N.; Andréasson, J.; Sundén, H. Multi-color emission with orthogonal input triggers from a diarylethene pyrene-OTHO organogelator cocktail. *ChemComm* **2020**, *56*, 988–991.
- (50) Mancini, R. S.; Lee, J. B.; Taylor, M. S. Boronic esters as protective groups in carbohydrate chemistry: processes for acylation, silylation and alkylation of glycoside-derived boronates. *Org. Biomol. Chem.* **2017**, *15*, 132–143.
- (51) Bérubé, M.; Dowlut, M.; Hall, D. G. Benzoboroxoles as efficient glycopyranoside-binding agents in physiological conditions: structure and selectivity of complex formation. *J. Org. Chem.* **2008**, *73*, 6471–6479.
- (52) Marinaro, W. A.; Schieber, L. J.; Munson, E. J.; Day, V. W.; Stella, V. J. Properties of a model aryl boronic acid and its boroxine. *J. Pharm. Sci.* **2012**, *101*, 3190–3198.
- (53) Sporzynski, A.; Leszczynski, P. Solubility of phenylboronic compounds in water. *Mediterr. J. Chem.* **2017**, *6*, 200–207.
- (54) Liu, J.; Fang, L.; Liu, C. Investigating the influences of intermolecular interactions on viscoelastic performance of pressure-sensitive adhesive by FT-IR spectroscopy and molecular modeling. *Drug Dev. Ind. Pharm.* **2020**, *46*, 1005–1014.
- (55) Huber, C.; Jahromy, S. S.; Birkelbach, F.; Weber, J.; Jordan, C.; Schreiner, M.; Harasek, M.; Winter, F. The multistep decomposition of boric acid. *Energy Sci. Eng.* **2020**, *8*, 1650–1666.
- (56) Bains, G. K.; Kim, S. H.; Sorin, E. J.; Narayanaswami, V. The extent of pyrene excimer fluorescence emission is a reflector of distance and flexibility: analysis of the segment linking the LDL receptor-binding and tetramerization domains of apolipoprotein E3. *Biochem.* **2012**, *51*, 6207–6219.